

1 Formation of cratonic lithosphere during the initiation of
2 plate tectonics

3 **A.P. Beall^{1*}, L. Moresi¹, and C.M. Cooper²**

4 *¹School of Earth Sciences, University of Melbourne, Parkville, Victoria 3010, Australia*

5 *²School of the Environment, Washington State University, PO Box 642812, Pullman,*
6 *Washington 99164-2812, USA*

7 **Current address: School of Earth & Ocean Sciences, Cardiff University, Cardiff CF10*
8 *3AT, UK*

9 **ABSTRACT**

10 The Earth's oldest near-surface material, the cratonic crust, is typically underlain
11 by thick lithosphere (>200 km) of Archean age. This cratonic lithosphere likely thickened
12 in a high compressional stress environment, potentially linked to the onset of crustal
13 shortening in the Neoproterozoic. Mantle convection in the hotter Archean Earth would have
14 imparted relatively low stresses on the lithosphere, whether or not plate tectonics was
15 operating, so a high stress signal from the early Earth is paradoxical. We propose that a
16 rapid transition, from heat-pipe mode convection to the onset of plate tectonics, generated
17 the high stresses required to thicken the cratonic lithosphere. Numerical calculations are
18 used to demonstrate that an existing buoyant and strong layer, representing depleted
19 continental lithosphere, can thicken and stabilize during a lid-breaking event. The peak
20 compressional stress experienced by the lithosphere is 3–4x higher than for the stagnant
21 lid or mobile lid regimes immediately before and after. It is plausible that the cratonic
22 lithosphere has not been subjected to this high stress-state since, explaining its long-term

23 stability. The lid-breaking thickening event reproduces features observed in typical
24 Neoproterozoic cratons, such as lithospheric seismological reflectors and the formation of
25 thrust faults. Neoproterozoic 'pre-tectonic' structures can also survive the lid-breaking
26 event, acting as strong rafts, that are assembled during the compressive event. Together,
27 the results indicate that the signature of a catastrophic switch, from a stagnant lid Earth to
28 the initiation of plate tectonics, has been captured and preserved in the characteristics of
29 cratonic crust and lithosphere.

30 INTRODUCTION

31 The surviving remnants of the Archean crust appear to have been formed under
32 conditions of a low geothermal gradient (Burke and Kidd, 1978) best explained by a pre-
33 plate tectonic, stagnant, heat-pipe mode of mantle convection characterized by vertical
34 tectonics and low convective stresses (Moore and Webb, 2013; Rozel et al., 2017). This
35 crust is underlain by the thickened remnants of lithosphere of similar age (Pearson et al.,
36 1995; O'Reilly et al., 2001) that form the stable, buoyant continental tectosphere (Jordan,
37 1975). Long term stability of the cratonic lithosphere requires high strength in addition to
38 buoyancy to survive erosion by mantle convection (Lenardic and Moresi, 1999). We
39 propose that cratons formed above regions of lithospheric foundering, predicted to have
40 occurred when the Earth switched from the heat-pipe mode to a mobile-lid, plate tectonic
41 regime (Moresi and Solomatov, 1998). We argue that stresses of this magnitude have not
42 been reproduced since the Archean, explaining the long-term mechanical stability of the
43 cratons and lack of modern examples.

44 The initial stability of the cratonic lithosphere requires high compressive stresses
45 (Cooper et al., 2006) to overcome its strength and buoyancy to thicken it to the now

46 observed 200–300 km (Pasyanos et al., 2014), which cannot be generated by any steady-
47 state Archean mantle regime. Mobile lid convection involves heat-loss through strong
48 oceanic geothermal gradients, as a result of surface migration and recycling,
49 characteristic of plate tectonics. In its absence, convection operates in the stagnant lid
50 mode (Moresi and Solomatov, 1998), which is dominated by conduction through a
51 globally uniform boundary layer (lid). The heat-pipe regime is a variant of this stagnant
52 lid mode, in which upward melt transport into and through the lid is the dominant heat-
53 loss mechanism and can generate continental crust and highly depleted lithosphere
54 (Moore and Webb, 2013; Rozel et al., 2017), consistent with the observed cratonic
55 composition (O'Reilly et al., 2001). However, this lithosphere would initially have a
56 modest thickness, consistent with estimated melting depths of <100 km (Lee, 2014). An
57 additional thickening mechanism is therefore required.

58 Cratonic mantle lithosphere thickening appears to have occurred through thrusting
59 analogous to plate tectonic collisional zones (Bostock, 1998), also observed in
60 Neoproterozoic crustal deformation (Percival et al. 2006). Once plate tectonics begins, the
61 mobile lid regime is able to generate higher stresses than the heat-pipe regime, but
62 subduction zone and convective stresses would still be significantly lower in the warmer
63 Archean mantle compared to today (van Hunen and van den Berg, 2008; Sandu et al.,
64 2011). Cratonic lithosphere formed as a result of thickening by steady-state mobile lid
65 convection is potentially unstable to rising mantle stresses over time in a cooling Earth
66 (Cooper et al. 2007). A transient, high-stress event occurring during the early mobile lid
67 regime is therefore required to thicken and stabilize strong lithosphere that can sustain
68 stability for billions of years.

69 The last significant recorded cratonic deformation (Percival et al., 2006; Van
70 Kranendonk et al., 2007) typically occurred at a similar time (within 300 Ma) to the
71 proposed initiation of plate tectonics at ~3 Ga (based on data summarized by
72 Hawkesworth et al., 2017). This switch from the heat-pipe regime to mobile lid (plate
73 tectonics) would momentarily generate extremely high stresses, as the heat-pipe thermal
74 boundary layer was catastrophically recycled into the mantle (Moore and Webb, 2013).
75 This paper examines the manner in which proto-crust and depleted lithosphere thicken
76 and stabilize during lid collapse and the transition to mobile-lid convection, forming
77 cratonic nuclei of considerable strength.

78 **DYNAMIC MODELING**

79 We solve Stokes flow and temperature advection-diffusion using Underworld in a
80 2D, Cartesian domain 8700×2900 km in size (Moresi et al., 2007, see the GSA Data
81 Repository for further details of the numerical modeling methodology). We modeled
82 internally heated whole mantle convection (Fig. 2), with a Rayleigh number (Ra) of
83 5×10^8 , a viscosity range of five orders of magnitude and a resolution of 12 km in the
84 horizontal direction. In the vertical direction, the upper mantle grid spacing is refined to
85 6km.

86 Our models begin with a 72.5 km harzburgite layer with a density of 3269
87 kg/m^{-3} (relative to an assumed mantle density of 3310 kg/m^3), consistent with
88 xenoliths (O'Reilly et al., 2001). Our focus is the dependence of craton stability on the
89 deep lithospheric buoyancy and strength. The influence of the continental crust, which
90 could have formed previously through melting and recycling through the heat-pipe lid, is
91 generally ignored. The lithosphere has a finite plastic strength modeled by a depth-

92 dependent Von Mises criterion, representing the increased strength of olivine at high
93 pressure (Karato, 2010) and is assumed to be dry and melt-depleted compared to the
94 mantle which is 8x weaker. The stagnant lid can only be recycled if its strength is limited
95 by a low yield stress of 10-50 MPa (as in Moresi and Solomatov, 1998), which can be
96 generated through dynamic grain-size reduction and a subsequent switch to diffusion
97 creep (Rozel, 2012). A yield strength of 0.6 MPa/km is set, assuming that this weakening
98 has occurred. A short damage-dependent model demonstrates that the lid-breaking event
99 and craton stabilization occur in a similar way without this simplification (data
100 repository).

101 Melting buffers the mantle temperature, which is approximated by capping the
102 geotherm at the depth-dependent solidus. This produces an intermediate geotherm which
103 lies between the cool, extrusive heat-pipe end member (Moore and Webb, 2013) and the
104 warmer, intrusive end-member (Rozel et al., 2017). When the mantle cools down
105 sufficiently for melting to switch off (following Moore and Webb, 2013), the lithospheric
106 thickness is no longer controlled by the solidus and a large wavelength lithosphere-
107 asthenosphere boundary (LAB) slope can form, typical of the stagnant lid regime (Moresi
108 and Solomatov, 1998). This LAB slope is associated with high stresses which trigger an
109 overturn event, subjecting the harzburgitic layer to an episode of high compressive stress
110 (Figs. 1 and 2). The continental layer is shortened by <80% to form <300 km thick
111 'cratonic nuclei' during the foundering event.

112 **STRESS HISTORY AND STABILITY OF THE CRATONIC LITHOSPHERE**

113 The lid-breaking event is associated with high horizontal compressional stresses
114 of ~150MPa in the buoyant lithosphere above the zones of mantle downwelling (Fig. 1).

115 These maximum stresses are 3–3.5x higher than the heat-pipe and stagnant lid regimes
116 (~30 MPa) prevailing immediately before the initiation of lid-breaking and the mobile lid
117 (plate tectonics) regime that follows.

118 The lid is recycled (except the continental layer) in fragments initially 1500km -
119 2000 km wide. Each produces a local stress pulse which lasts 10-50Ma and contributes to
120 the formation of localized shear zones and thrust stacking within the cratonic lithosphere.
121 Thrusting occurs locally until the cratonic lithosphere stabilizes, incrementally
122 assembling a complete craton with up to three pulses over 100 - 350 Ma (central craton in
123 Figure 2B; one pulse has generated a single nucleus by 193 Ma and two more by 609
124 Ma), predicting in a wide range of craton formation ages globally. Due to the lithospheric
125 strength at high pressure and its cold pre-tectonic geotherm, stabilization occurs as soon
126 as the lithosphere is thickened to a critical depth (as in Cooper et al. 2006). No further
127 cooling or annealing mechanisms are required for stability, which would require longer
128 lived compressional regimes than typical for the hotter mantle.

129 Once all of the cold, dense lower lid has been recycled, no subsequent high stress
130 pulses occur, as a thick boundary layer can no longer form in the mobile lid (plate
131 tectonics) regime. Models are run for ~500 Ma after the lid-breaking event, in which the
132 modeled craton stress remains below ~30% of the thickening stress. The cratons remain
133 stable within the convecting mobile lid regime (e.g., craton stability after 609 Ma, Fig.
134 2B), despite an initial period of craton warming and mantle cooling.

135 The stress state evolution from the modeled Archean mobile lid convection to the
136 modern Earth is estimated by scaling convective stress as a function of mantle
137 temperature, which is estimated to have cooled by ~200 °C (Herzberg et al., 2010).

138 Mobile lid convective stress varies in proportion to the mantle viscosity (the Frank-
139 Kamenetskii approximation of temperature-dependence is assumed, with $E = 12$) and
140 the convective boundary layer thickness which scales with $Ra^{-\frac{1}{3}}$ (Turcotte and Oxburgh,
141 1972; Moresi and Solomatov, 1998). This scaling predicts modeled stresses which are
142 2.5x higher (~75 MPa) in the modern Earth than in the Archean (Fig. 1). The modern
143 cratonic lithospheric stress-state would therefore have only reached ~60%–80% of the
144 stress experienced during its Archean thickening event.

145 The maximum lithospheric stress during Earth’s evolution over the last 3 Ga
146 should also be reflected in the evolution of maximum orogenic crustal thickness. The
147 maximum thickness of orogenic crust is limited to isostatic equilibrium with its local
148 compressional stress state. The largest crustal thickness is proportional to the highest
149 tectonic stress and provides an upper bound for the cratonic lithosphere stress state.
150 Dhuime et al. (2015) calculated the billion year evolution of juvenile upper-plate
151 continental crust thickness at subduction zones, based on geochemical isotopic
152 compilations, which we use as a proxy for tectonic stress. After ~3Ga, stresses increased
153 by 2.2x by ~1.5 Ga, which is initially more rapid than the scaling estimate (Fig. 1).
154 However, the subduction zone stress peaked at this time, such that it is still only ~70% of
155 the stress experienced during craton formation.

156 The simplified stress evolution is also consistent with the mantle traction stresses
157 and lithospheric stress due to topography (<50 MPa) and net lithospheric stresses near
158 subduction zones (~100 Mpa, Lithgow-Bertolloni and Guynn, 2004). This estimate
159 depends on the lithosphere-mantle stress balance, without which subduction traction
160 could theoretically generate <200 Mpa.

161 These stress estimates support our hypothesis that the high lithospheric stresses
162 which built the cratons have not been reproduced since their formation. The thermal
163 boundary layer may have thickened, but the cratonic nuclei are predicted to be
164 undeformed unless weakened. The importance of weakening cratons through slab-derived
165 fluid influx is debatable (Lee et al. 2011). The calculated stress evolution indicates that
166 weakening was critical in the past, though subduction zone traction stresses may have
167 risen to magnitudes for which this may be becoming less necessary in anomalously high
168 stress regions.

169 **PRESERVATION OF PRE-PLATE TECTONICS CRUST**

170 The simplified numerical model is an end-member in which the buoyancy and
171 strength of continental crust is negligible. A strong compressional stress-state consistent
172 with both shallow and deep thrusting is generated (Fig. 2 and Cooper et al., 2006).
173 Thrusting is recorded in Neoproterozoic crustal structures (e.g., Yilgarn and Superior
174 cratons; van der Velden et al., 2006; Percival et al., 2006), but its absence is a key
175 characteristic of Paleoproterozoic crust. Cratonic nuclei which formed >3 Ga (Pilbara and
176 Kaapvaal cratons) are instead dominated by buoyancy-driven domes (Van Kranendonk et
177 al., 2007), with no evidence of craton thickening. This can be explained by assuming that
178 lid breaking events generated the earliest thrusting and only occurred post-3Ga, which
179 agrees with the predicted onset of tectonics (Hawkesworth et al., 2017) and allows
180 Paleoproterozoic crust sufficient time to have ‘stabilized’. Additional models (Fig. 2d) test
181 this by including an embedded 580 x 36.25 km crustal fragment of Paleoproterozoic crust,
182 stronger and more buoyant than the continental lithosphere with a plastic strength of 1.5
183 MPa/km and a density of 2877 kg/m^{-3} .

184 The buoyancy of the crustal block, applicable to felsic crust of any age, prevents
185 its deep burial. It is transported onto thick cratonic lithosphere (Fig. 2d) with no internal
186 plastic deformation and relatively modest viscous thickening (which would be further
187 reduced if strain-localization were modeled). Neoproterozoic crust was forming and
188 therefore still weak enough for the lid-breaking event to generate thrusts (preserved as a
189 synmagmatic combination of horizontal and vertical tectonics in the Yilgarn, Zibra et al.,
190 2014). The structural and geochemical contrasts, for example between Yilgarn and
191 Pilbara crust, may then be the consequence of the large-scale convective regime they
192 formed in, whereas their lithospheric roots formed through similar thickening processes
193 during the initiation of tectonics.

194 **EVIDENCE IN THE GEOLOGICAL RECORD**

195 While our cratonization models are primarily designed to reconcile mantle regime
196 dynamics with the mechanical properties of the cratons, they also reproduce observed
197 features of cratons. Thrusting of the lithosphere and displacement of internal layering on
198 a large scale occurs in the models and can reproduce observed dipping lithospheric
199 reflectors (Bostock, 1998), as well as mid-lithospheric discontinuities (Calò et al., 2016).
200 Rapid Neoproterozoic events involving the amalgamation of multiple cratonic nuclei
201 (Percival et al., 2006) can also be generated by the lid breaking episode, which provides a
202 mechanism for suturing terranes in a relatively low stress tectonic environment. In the
203 models, individual mantle downwellings generate cratonic nuclei and suture them to form
204 larger assembled cratons. This has the combined effect of transporting crust laterally by
205 <4000 km, suturing terranes which would have contrasting geological evolution due to
206 their initial isolation, as observed in the Superior Province (Percival et al., 2006). Finally,

207 Neoproterozoic crust preserves horizontal tectonic features which can be explained by the
208 lid-breaking mechanism. The thrust sheets would reflect the compressional stress-state
209 (described earlier). Late-stage felsic magmatism (Percival et al., 2006) could be generated
210 as hydrated mafic crust was rapidly buried to >100 km (Fig. 1, Bédard, 2006), the
211 displacement also assisting with its recycling through the lithosphere.

212 The strongest evidence for craton formation during a catastrophic mantle
213 transition is the anomalous thickness, strength and billion year stability of the preserved
214 cratonic lithosphere, which places constraints on the evolving mantle dynamics since the
215 Archean. These features are reconcilable with craton formation during the proposed lid-
216 breaking event, which would have generated a pulse of high stress, anomalous compared
217 to lithospheric stresses generated both during the Archean and today. The lid-breaking
218 event involves strong coupling between the asthenosphere, mantle lithosphere and crust,
219 providing opportunities to support our hypothesis with Archean crustal observations. The
220 simplified models demonstrate that our craton formation model is plausible, while there
221 is now the opportunity to more thoroughly explore the role of dynamic rheology and
222 crustal deformation. The lid-breaking model provides a plausible framework for
223 interpreting unique Neoproterozoic lithospheric and crustal features, which are otherwise
224 difficult to explain purely with secular adjustment to modern-style subduction and plate
225 tectonic models.

226 **ACKNOWLEDGMENTS**

227 This research was supported by the Geological Survey of Western Australia (AB).
228 It was undertaken with the assistance of resources from the Pawsey Supercomputing
229 Centre, which operates with funding from the Australian Government and the

230 Government of Western Australia. We thank P. Cawood and C. Hawkesworth for their
231 discussions and T. Gerya, J. van Hunen and F. Cramer for their constructive reviews.

232 **REFERENCES CITED**

233 Bédard, J.H., 2006, A catalytic delamination-driven model for coupled genesis of
234 Archaean crust and sub-continental lithospheric mantle: *Geochimica et*
235 *Cosmochimica Acta*, v. 70, p. 1188–1214, <https://doi.org/10.1016/j.gca.2005.11.008>.

236 Bostock, M.G., 1998, Mantle stratigraphy and evolution of the Slave province: *Journal of*
237 *Geophysical Research. Solid Earth*, v. 103, p. 21183–21200,
238 <https://doi.org/10.1029/98JB01069>.

239 Burke, K., and Kidd, W.S.F., 1978, Were Archean continental geothermal gradients
240 much steeper than those of today?: *Nature*, v. 272, p. 240–241,
241 <https://doi.org/10.1038/272240a0>.

242 Calò, M., Bodin, T., and Romanowicz, B., 2016, Layered structure in the upper mantle
243 across North America from joint inversion of long and short period seismic data:
244 *Earth and Planetary Science Letters*, v. 449, p. 164–175,
245 <https://doi.org/10.1016/j.epsl.2016.05.054>.

246 Cooper, C.M., Lenardic, A., Levander, A., and Moresi, L., 2006, Creation and
247 preservation of cratonic lithosphere: Seismic constraints and geodynamic models, *in*
248 Benn, K., et al., eds., *Archean Geodynamics and Environments*: American
249 Geophysical Union, *Geophysical Monograph Series*, v. 164, p. 75–88.

250 Dhuime, B., Wuestefeld, A., and Hawkesworth, C.J., 2015, Emergence of modern
251 continental crust about 3 billion years ago: *Nature Geoscience*, v. 8, p. 552–555,
252 <https://doi.org/10.1038/ngeo2466>.

- 253 Hawkesworth, C.J., Cawood, P.A., Dhuime, B., and Kemp, T.I., 2017, Earth's
254 Continental Lithosphere Through Time: Annual Review of Earth and Planetary
255 Sciences, v. 45, p. 169–198, <https://doi.org/10.1146/annurev-earth-063016-020525>.
- 256 Herzberg, C., Condie, K., and Korenaga, J., 2010, Thermal history of the Earth and its
257 petrological expression: Earth and Planetary Science Letters, v. 292, p. 79–88,
258 <https://doi.org/10.1016/j.epsl.2010.01.022>.
- 259 van Hunen, J., and van den Berg, A.P., 2008, Plate tectonics on the early Earth:
260 Limitations imposed by strength and buoyancy of subducted lithosphere: Lithos,
261 v. 103, p. 217–235, <https://doi.org/10.1016/j.lithos.2007.09.016>.
- 262 Jordan, T.H., 1975, The continental tectosphere: Reviews of Geophysics, v. 13, p. 1–12,
263 <https://doi.org/10.1029/RG013i003p00001>.
- 264 Karato, S.I., 2010, Rheology of the deep upper mantle and its implications for the
265 preservation of the continental roots: A review: Tectonophysics, v. 481, p. 82–98,
266 <https://doi.org/10.1016/j.tecto.2009.04.011>.
- 267 Lee, C.T.A., Luffi, P., and Chin, E.J., 2011, Building and destroying continental mantle:
268 Annual Review of Earth and Planetary Sciences, v. 39, p. 59–90,
269 <https://doi.org/10.1146/annurev-earth-040610-133505>.
- 270 Lee, C.T.A. and Chin, E.J., 2014. Calculating melting temperatures and pressures of
271 peridotite protoliths: Implications for the origin of cratonic mantle. Earth and
272 Planetary Science Letters, v. 403, p. 273-286,
273 <https://doi.org/10.1016/j.epsl.2014.06.048>

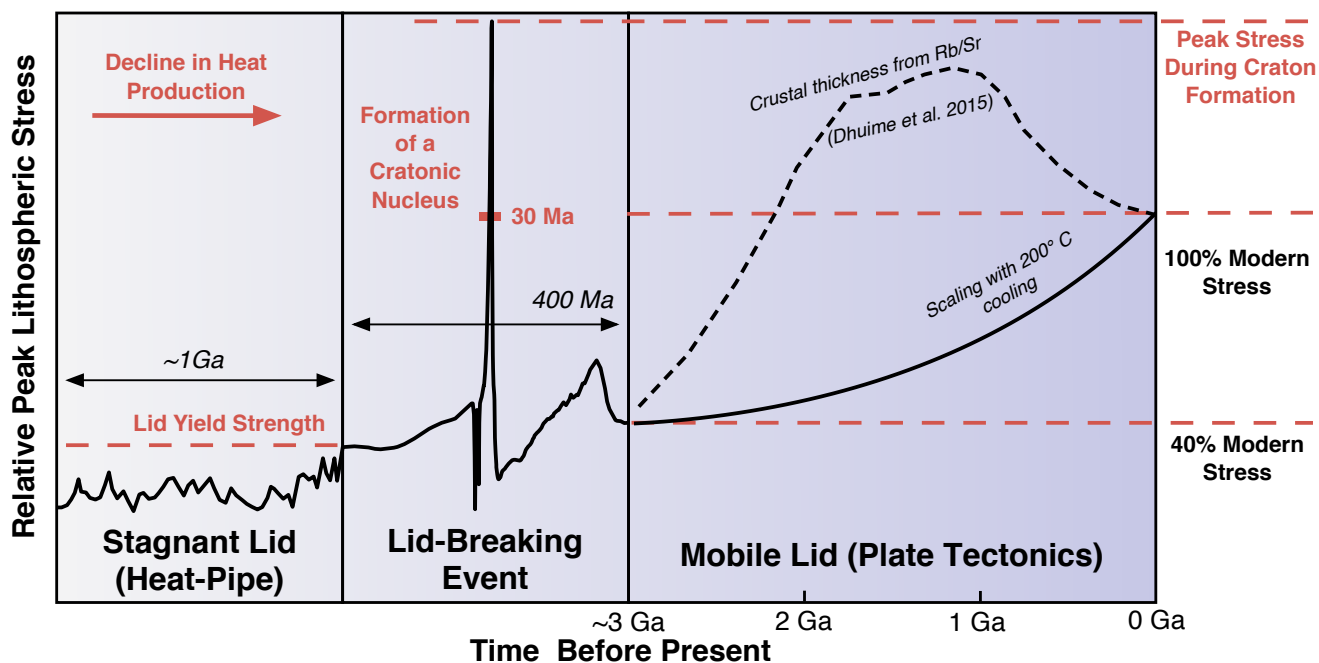
- 274 Lenardic, A., and Moresi, L.N., 1999, Some thoughts on the stability of cratonic
275 lithosphere: Effects of buoyancy and viscosity: *Journal of Geophysical Research.*
276 *Solid Earth*, v. 104, p. 12747–12758, <https://doi.org/10.1029/1999JB900035>.
- 277 Lithgow-Bertelloni, C. and Guynn, J.H., 2004. Origin of the lithospheric stress field.
278 *Journal of Geophysical Research: Solid Earth*, v. 109,
279 <https://doi.org/10.1029/2003JB002467>.
- 280 Moore, W.B., and Webb, A.A.G., 2013, Heat-pipe earth: *Nature*, v. 501, p. 501,
281 <https://doi.org/10.1038/nature12473>.
- 282 Moresi, L., and Solomatov, V., 1998, Mantle convection with a brittle lithosphere:
283 thoughts on the global tectonic styles of the Earth and Venus: *Geophysical Journal*
284 *International*, v. 133, p. 669–682, <https://doi.org/10.1046/j.1365-246X.1998.00521.x>.
- 285 Moresi, L., Quenette, S., Lemiale, V., Meriaux, C., Appelbe, B., and Mühlhaus, H.B.,
286 2007, Computational approaches to studying non-linear dynamics of the crust and
287 mantle: *Physics of the Earth and Planetary Interiors*, v. 163, p. 69–82,
288 <https://doi.org/10.1016/j.pepi.2007.06.009>.
- 289 O'Reilly, S.Y., Griffin, W.L., Poudjom Djomani, Y.H., and Morgan, P., 2001, Are
290 lithospheres forever: Tracking changes in subcontinental lithospheric mantle through
291 time: *GSA Today*, v. 11, p. 4–10, [https://doi.org/10.1130/1052-](https://doi.org/10.1130/1052-5173(2001)011<0004:ALFTCI>2.0.CO;2)
292 [5173\(2001\)011<0004:ALFTCI>2.0.CO;2](https://doi.org/10.1130/1052-5173(2001)011<0004:ALFTCI>2.0.CO;2).
- 293 Pasyanos, M.E., Masters, T.G., Laske, G., and Ma, Z., 2014, LITHO1. 0: An updated
294 crust and lithospheric model of the Earth: *Journal of Geophysical Research. Solid*
295 *Earth*, v. 119, p. 2153–2173, <https://doi.org/10.1002/2013JB010626>.

- 296 Pearson, D.G., Carlson, R.W., Shirey, S.B., Boyd, F.R., and Nixon, P.H., 1995,
297 Stabilisation of Archaean lithospheric mantle: A ReOs isotope study of peridotite
298 xenoliths from the Kaapvaal craton: *Earth and Planetary Science Letters*, v. 134,
299 p. 341–357, [https://doi.org/10.1016/0012-821X\(95\)00125-V](https://doi.org/10.1016/0012-821X(95)00125-V).
- 300 Percival, J.A., Sanborn-Barrie, M., Skulski, T., Stott, G.M., Helmstaedt, H., and White,
301 D.J., 2006, Tectonic evolution of the western Superior Province from NATMAP and
302 Lithoprobe studies: *Canadian Journal of Earth Sciences*, v. 43, p. 1085–1117,
303 <https://doi.org/10.1139/e06-062>.
- 304 Rozel, A., 2012, Impact of grain size on the convection of terrestrial planets, *Geochem.*
305 *Geophys. Geosyst.*, v. 13, <https://doi.org/10.1029/2012GC004282>.
- 306 Rozel, A.B., Golabek, G.J., Jain, C., Tackley, P.J., and Gerya, T., 2017, Continental crust
307 formation on early Earth controlled by intrusive magmatism: *Nature*, v. 545, p. 332–
308 335, <https://doi.org/10.1038/nature22042>.
- 309 Sandu, C., Lenardic, A., O'Neill, C.J., and Cooper, C.M., 2011, Earth's evolving stress
310 state and the past, present, and future stability of cratonic lithosphere: *International*
311 *Geology Review*, v. 53, p. 1392–1402,
312 <https://doi.org/10.1080/00206814.2010.527672>.
- 313 Turcotte, D.L., and Oxburgh, E.R., 1972, Mantle convection and the new global
314 tectonics: *Annual Review of Fluid Mechanics*, v. 4, p. 33–66,
315 <https://doi.org/10.1146/annurev.fl.04.010172.000341>.
- 316 Van Kranendonk, M.J., Hugh Smithies, R., Hickman, A.H., and Champion, D.C., 2007,
317 Secular tectonic evolution of Archean continental crust: interplay between horizontal

318 and vertical processes in the formation of the Pilbara Craton, Australia: *Terra Nova*,
319 v. 19, p. 1–38, <https://doi.org/10.1111/j.1365-3121.2006.00723.x>.
320 van der Velden, A.J., Cook, F.A., Drummond, B.J., and Goleby, B.R., 2006, Reflections
321 of the Neoproterozoic: A global perspective, *in* Benn, K., et al., eds., *Archean*
322 *Geodynamics and Environments*: American Geophysical Union, Geophysical
323 Monograph Series, v. 164, p. 255–265.
324 Zibra, I., Gessner, K., Smithies, H.R., and Peternell, M., 2014, On shearing, magmatism
325 and regional deformation in Neoproterozoic granite-greenstone systems: Insights from
326 the Yilgarn Craton: *Journal of Structural Geology*, v. 67, p. 253–267,
327 <https://doi.org/10.1016/j.jsg.2013.11.010>.

328

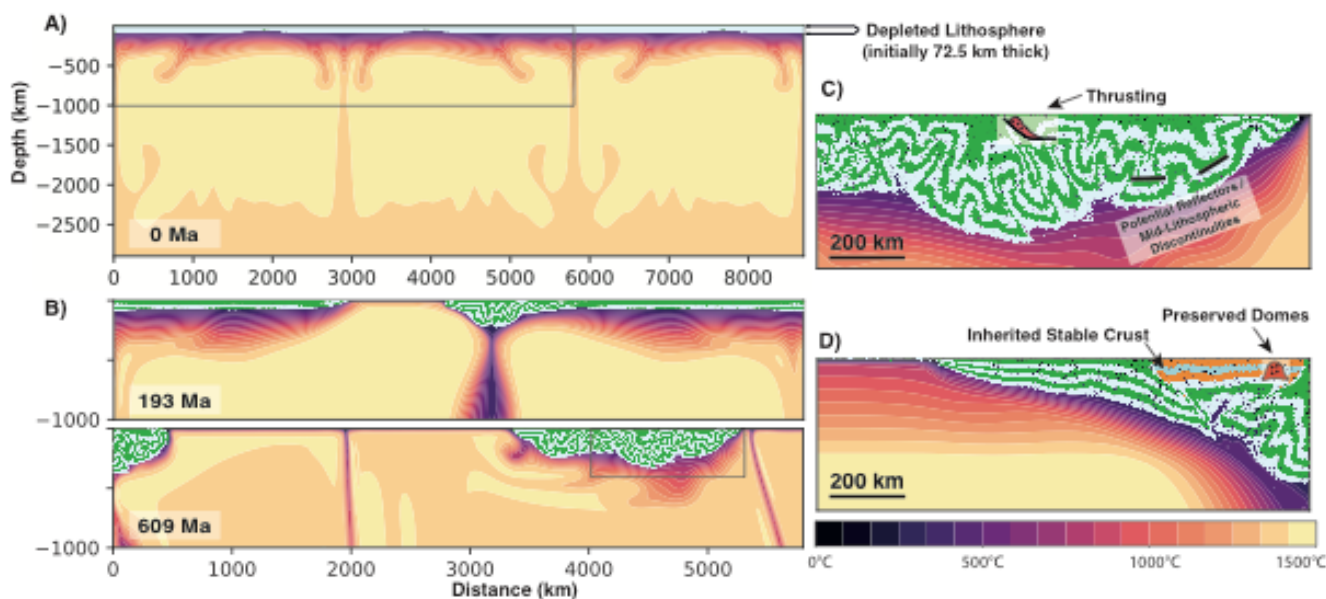
329 **FIGURES**



330

331

332 Figure 1. Earth's evolving lithospheric stress state. The maximum stress during the
333 modeled stagnant lid regime is relatively low and increases gradually due to declining
334 heat-production. When widespread melting switches off, the stagnant lid can develop a
335 boundary layer slope and stresses increase rapidly, reaching the stagnant lid yield stress
336 and triggering the lid-breaking event and the initiation of plate tectonics, at ~3Ga
337 (Hawkesworth et al., 2017). Archean tectonic stresses are likely to be ~60% smaller than
338 today, based on the variation of crustal thickness over time (Dhuime et al. 2015) and
339 mantle convection scaling with $200^{\circ}C$ of cooling. The modeled lid-breaking event
340 generates pulses of anomalously high stress (ranging <300 Ma after lid-breaking) which
341 form strong cratonic nuclei. These anomalous stresses have not been reproduced since.
342 The lid-breaking event explains cratonic lithosphere formation in an otherwise low-stress
343 environment and the following stability at the billion year time-scale.
344



345
346 Figure 2. Typical model evolution from the stagnant lid regime (A), to the initiation of
347 the lid-breaking event and stabilization of thick cratonic lithosphere (B, note scale

348 change). The maximum stress evolution of the left craton is shown in Figure 1 (central
349 panel) and is representative. The data repository contains a movie of this model and the
350 stress evolution for the other two cratons. Individual thickening events take <30 Ma,
351 while multiple cratonic nuclei are amalgamated into the large central craton within 100
352 Ma. An enlarged frame of the thickened lithosphere (C) demonstrates the thrust structures
353 preserved after thickening. (D) An embedded Palaeoarchean crustal fragment, assumed to
354 have stabilized before the lid-breaking event, records relatively small shortening. This
355 explains the preservation of vertical tectonic structures, whereas significant thrusting
356 occurs in the weaker Neoproterozoic crust (shown schematically).
357
358 1GSA Data Repository item 2018xxx, further details of numerical modeling
359 methodology and movie of typical model evolution, is available online at
360 <http://www.geosociety.org/datarepository/2018/> or on request from
361 editing@geosociety.org.